

Developmental maturation of hepatic n-3 polyunsaturated fatty acid metabolism: Supply of docosahexaenoic acid to retina and brain

Rex E. Martin, Elena B. Rodriguez de Turco, and Nicolas G. Bazan

LSU Eye Center and Neuroscience Center, Louisiana State University Medical Center, New Orleans, LA USA

Docosahexaenoic acid is an essential fatty acid enriched in lipids of photoreceptor, synaptic, and nerve growth cone membranes. [³H]docosahexaenoic acid was intraperitoneally injected in 5-day-old and 14-day-old mouse pups, and the labeling time course was followed in liver, plasma, brain, and retina for 72 hours. The liver of 5-day-old mice displayed higher content and labeling of triacylglycerols, lower content of phospholipids, and a more avid uptake of [³H]docosahexaenoic acid as compared with 14-day-old mice. Maximal [³H]docosahexaenoic acid labeling in the liver was observed 2 hr postinjection and decreased thereafter as [³H]docosahexaenoic acid accumulated in brain and retina. The most efficient [³H]docosahexaenoic acid accumulation in retina and brain occurred with 14-day-old pups and correlated with a higher labeling and a long half-life of [³H]docosahexaenoic acid phospholipids in liver (35 hr for 5-day-olds and 54 hr for 14-day-olds) and plasma (42 hr for 5-day-olds and 68 hr for 14-day-olds). As a function of time, the labeling profile in plasma lipids followed that of liver. A significant amount of total plasma docosahexaenoic acid was found esterified into cholesterol esters, while docosahexaenoic acid-phospholipids accounted for 60 to 70% at both ages. Docosahexaenoic acid cholesterol ester may also be a carrier of docosahexaenoic acid to neural tissues after synthesis in the liver and/or in high density lipoproteins from a liver-derived docosahexaenoic acid-phosphatidylcholine pool. Both cholesterol and docosahexaenoic acid are needed for neural membrane biogenesis. Collectively, these data indicate that the metabolism of docosahexaenoic acid by liver and the uptake and esterification of docosahexaenoic acid into hepatic lipids and its subsequent appearance in the plasma are developmentally regulated and under control by the liver. The esterification of docosahexaenoic acid into phospholipids and the increased half-life of [³H]docosahexaenoic acid-phospholipids in plasma may be salient factors modulating efficient docosahexaenoic acid delivery to the central nervous system. (J. Nutr. Biochem. 5:151–160, 1994.)

Keywords: docosahexaenoic acid; photoreceptors; liver; n-3 fatty acids; brain; retina

Introduction

Docosahexaenoic acid (DHA, 22:6), an omega-3 (n-3) fatty acid, is present in unusually high concentrations in phospholipids (PL) from retina,^{1,2} brain,³ and testes.⁴ DHA is im-

portant for development and function of the central nervous system (CNS).^{5–10} In fact, DHA is preferentially incorporated in nerve growth cone membranes¹¹ and photoreceptors.¹² Moreover, impairments in the electroretinograms,^{13–15} in visual acuity,^{5,14} and in learning ability^{16,17} are correlated with dietary deprivation of n-3 fatty acids.

Because mammals lack the enzymes necessary for de novo DHA synthesis, DHA is derived either directly from the diet or synthesized from dietary n-3 precursors such as α -linolenic acid (18:3n-3).^{18,19} These precursors are enriched in plants, and an abundant source of DHA is fish oil.²⁰ In early postnatal life, the phospholipids of milk provide significant amounts of DHA required by developing infants.⁹

DHA accumulation in retina and brain during development is related to the diet^{7,21,22} and to "tissue-specific" factors. The

This work was supported in part by the National Institutes of Health, EY02377 and EY04428.

Present address for Dr. Martin is The University of Oklahoma Health Sciences Center, College of Medicine, Department of Anatomical Sciences, Oklahoma City, OK 73104 USA.

Address reprint requests to Dr. Nicolas G. Bazan at the Louisiana State University Medical Center School of Medicine, LSU Eye Center and Neuroscience Center, 2020 Gravier Street, Suite B, New Orleans, LA 70112 USA.

Received July 19, 1993; accepted October 12, 1993.

retina and brain synthesize DHA from dietary precursors (18:3 n-3),^{19,23-25} although the liver has a very high capacity for DHA synthesis.^{26,27} The retina conserves DHA during periods of n-3 fatty acid deprivation,^{14,28-30} and dietary n-3 fatty acids depletion diminishes DHA content in liver, heart, and testes, but not in brain.³¹ In the rodent, the activity of the first enzyme involved in the conversion of 18:3n-3 to DHA (Δ -6 desaturase) increases postnatally in the liver while it decreases in brain.^{26,32} The liver also displays developmental changes in lipogenesis and in its ability to secrete lipoproteins.^{33,34} The DHA supply to the nervous tissue is through lipoproteins from the liver, comprising an efficient route to meet the demands for the fatty acid by those tissues.^{27,35-37} This route operates throughout life, but is upregulated during active synapse and photoreceptor biogenesis in postnatal development.²⁷ The liver, therefore, assembles and secretes lipoproteins with phospholipids containing DHA.^{35,38} In the neural tissue, DHA is likely taken up by receptor-mediated mechanisms.^{27,35,37} Subsequently, an intercellular route (short-loop) ensures DHA retention in the neural tissues.^{12,35,39}

The observation that most of the n-3 fatty acids of mouse pup stomach contents is 18:3n-3, whereas it is DHA in the plasma, led us to follow the fate of radiolabeled 18:3n-3 administered by intraperitoneal or percutaneous intragastric injection in 3-day-old (P3) mouse. The results provided strong evidence for the supply of DHA from liver to retina and brain after elongation and desaturation of its precursor.²⁷ Because DHA is the predominant n-3 fatty acid arriving through the circulation to the nervous tissue, we decided to assess [³H]DHA metabolism after systemic administration at two postnatal ages: at 5 days postnatal (P5), when there is active cell division and growth in the brain and inner segment of photoreceptors is developed in the retina, and at 14 days postnatal (P14), when active proliferation of dendrites and synaptogenesis occur and outer segment of photoreceptors starts to develop.⁴⁰ We addressed the following: (a) comparative metabolism at P5 and P14; (b) metabolism and endogenous fatty acid composition of liver and plasma lipids; and (c) arrival of [³H]DHA to retina and brain. Our results indicate that the long-loop route from liver to neural tissue through the blood stream operates during the postnatal development, mainly through DHA-phosphatidylcholine. Furthermore, our results support the hypothesis that delivery of DHA to the retina and brain is developmentally regulated and controlled by the liver.

Methods and materials

C57BL/6J mice from Jackson Laboratories (Bar Harbor, MN USA) were maintained in the Louisiana State University Medical Center animal care facility and fed mouse chow (Purina, St. Louis, MO USA) ad libitum for several generations. Animals were treated in accordance with guidelines established by the Association for Research in Vision and Ophthalmology (ARVO), and all experimental procedures were pre-approved by the L.S.U.M.C. Institutional Animal Care and Use Committee. Litters were reduced to eight pups after birth, and both sexes were used randomly.

[4, 5-³H]DHA (specific activity 17.9 Ci/mmol; New England Nuclear-DuPont, Boston, MA USA) was administered intraperitoneally (i.p.) as a sodium salt (3.33 μ Ci/g body weight) to mouse pups at P5 and P14. Following injection of [³H]DHA, mice were returned to their mothers until they were used. Individual litters

were used at each time point after injection (2, 6, 24, and 72 hr). Blood was collected in heparinized tubes via cardiac puncture and centrifuged at low speed to collect plasma. The eyes were enucleated and retinas were rapidly dissected from eyecups under ice-cold saline. Brain and liver were also collected, and each tissue was immediately homogenized in chloroform:methanol (2:1, vol/vol). Lipids were extracted and purified,⁴¹ and aliquots were taken for determination of total [³H]DHA and lipid phosphorus (P) content.⁴² Individual neutral lipids and phospholipids were isolated by thin layer chromatography (TLC) using monodimensional and bidimensional systems, respectively.⁴¹ Prior to radiochemical analysis, lipid spots were visualized with iodine and scraped into vials containing 1 mL of water. After adding 10 mL of Ready Gel (Beckman, Fullerton, CA USA), radioactivity in these spots was determined in a scintillation counter (Beckman).

Aliquots of purified lipid extracts were taken for high performance liquid chromatography (HPLC) analysis of radiolabeled acyl chains.⁴³ Gas-liquid chromatography (GLC) analysis of endogenous fatty acid content and composition was done for the total lipid extracts and for individual lipids isolated by TLC and identified with UV light after spraying the plate with 0.005% dichlorofluorescein in methanol.⁴¹ Acyl chains were derivatized to fatty acid methylesters by acid-catalyzed methanolysis for GLC analysis. Briefly, the extracts were dried under a stream of nitrogen in 13 \times 100 mm glass screw-top tubes, and 2 mL of toluene:methanol:sulfuric acid (100:100:4) was added to each tube. The tubes were capped under nitrogen with teflon septa and incubated with agitation for 4 hr at 65° C. The tubes were cooled to room temperature, and 1 mL of water, 3 mL of hexane, and known amounts of two internal standards (heptadecanoate and heneicosanoate) were added.

Statistical analysis

Values expressed as mole percent \pm SD and μ Ci per mg lipid phosphorus \pm SD were analyzed, as specified in figure and table legends, using a completely randomized design in the factorial analysis of variance (ANOVA).⁴⁴ In the first group of data, the mole percent of lipid was hypothesized to be accounted for by the following factors: age of the pups (P5 and P14), the type of lipid (CE, TAG, PL), and the fatty acid chain length and saturation. For the second group of data, the factors considered were: age of the pups (P5 and P14), the tissue samples (liver, plasma, brain, retina), the type of lipid (CE, FFA, PL, TAG, total lipids), and the time post-injection. The analysis was carried out using the SAS (SAS Institute, Cary, NC USA) programming language and procedures⁴⁵ on an IBM 3090 series mainframe computer (IBM, White Plains, NY USA). Comparisons between the means were accomplished using *t* tests between least square means generated from the design and based on pooled variances.⁴⁶ Other comparisons between P5 and P14 were done by paired Student's *t* test as stated in figure and table legends. Values were considered statistically significantly different when *P* < 0.05.

The half-lives were estimated from a linear regression analysis of log of labeling (μ Ci/mg lipid P) versus time (hours) post injection: {log(μ Ci/mgP) = *mt* + *b*}, using the equation half-life = log 2.0/*m*, where *m* is the slope of the line and *b* is the y-intercept.

Results

Lipid content and acyl chain composition in liver and plasma

Between P5 and P14, the average mouse body weight increased by 70% (3.6 \pm 0.3g to 6.1 \pm 0.3g). The wet weight of the livers increased only 39% (124 \pm 6mg to 172 \pm 22mg), while total lipid phosphorus increased by 81% (129 \pm 10 μ g

to $234 \pm 36 \mu\text{g}$). During this period of postnatal development, the total liver lipid content decreased due to a 90% decrease in triacylglycerol (TAG) content (Table 1). At the same time, liver PL content increased by 28%. At P5, TAG acyl chain content represented 65% of the total lipids in liver and 26% of the total hepatic DHA. In contrast, by P14, 96% of the total hepatic DHA was esterified into PL, but only 4% was esterified into TAG. Between P5 and P14, differences in concentration of TAG and PL in plasma followed trends similar to those of liver. At P5 the molar ratios of PL to TAG were 0.8 and 1.0 for plasma and liver, respectively, as compared with 11.7 and 3.5 at P14. Most of the DHA in plasma was in PL (61% at P5 and 68% at P14). As much as 21% of plasma DHA was esterified into triacylglycerol (TAG) at P5, while it decreased to 6% at P14. The contribution of the cholesterol ester (CE) fraction to total plasma DHA was also higher at P14 (24%) than at P5 (12%).

Age-related changes in the endogenous fatty acid composition of CE, TAG, and PL in liver and in plasma are shown in Tables 2 and 3. The most abundant unsaturated fatty acid in hepatic TAG and CE was oleic acid (18:1n-9), followed by linoleic acid (18:2n-6) and arachidonic acid (20:4n-6). By P14, the percent content of 18:1n-9 in TAG decreased, while the percent of the saturated fatty acids palmitic acid (16:0) and stearic acid (18:0) increased. The percent content of total n-6 and n-3 fatty acids in TAG remained unchanged between P5 and P14. However, at P14, higher proportions of docosapentaenoic acid (22:5n-6) and DHA concomitant with lower proportions of their precursors were noted. In hepatic PL, 20:4n-6 and DHA, followed by 18:1n-9 and 18:2n-6, were the most abundant fatty acids at P5. At P14, 20:4n-6 and 18:2n-6 were most abundant, followed by DHA and 18:1n-9. Minimal changes in the percent content of total n-6 and n-3 fatty acids were seen between P5 and P14. In plasma, TAG and PL acyl group composition followed profiles similar to liver (Table 3). The main unsaturated fatty acid present in TAG was 18:1n-9, while 18:2 and 20:4 prevailed in PL. Minimal differences were observed in the

acyl chain content of TAG between P5 and P14. However, at P14, PL displayed lower percent content of 20:4n-6 and 22:6n-3 and higher content of 18:2n-6 and 18:0. CE was the only lipid that showed higher content of n-6 and n-3 fatty acids in plasma than it did in the liver. Furthermore, n-6 fatty acids accounted for 47% and 58% of the total CE acyl groups. As was observed in the other lipid fractions, at P14, CE was enriched in 18:2n-6.

Hepatic uptake and metabolism of [^3H]DHA

No elongation or retroconversion of the intraperitoneally injected [^3H]DHA over 72 hr was apparent by HPLC analysis in liver, brain, or retina (data not shown), in agreement with previous observations.¹¹

Within 2 hr of [^3H]DHA injection, similar amounts of the radiolabeled fatty acid were observed in the livers of P5 and P14 pups (Table 4). The total label recovered accounted for 19% and 14%, respectively, of the injected fatty acid. During the next 70 hr, the apparent [^3H]DHA loss from the liver was similar for both age groups ($\approx 1.7 \mu\text{Ci/liver}$). This occurred as labeling of the brain and retina increased. Seventy-two hours post-injection the label recovered in these organs represented 24% (at P5) and 59% (at P14) of the total [^3H]DHA lost from liver between 2 hr and 72 hr.

Figure 1 compares total lipid labeling in liver, plasma, brain, and retina from P5 and P14 mice after [^3H]DHA injection. The liver showed higher labeling than the plasma at both ages and at all times examined. The early uptake of [^3H]DHA by the liver of P5 pups was 1.5-fold higher than at P14. The difference in labeling became similar by 72 hr postinjection. A similar 1.7-fold difference was observed between the two age groups in the endogenous hepatic DHA content (11 and 7 nmole/ μg total lipid P, at P5 and P14, respectively; values calculated from data in Table 1). While hepatic labeling decreased 52% between 2 hr and 24 hr after injection at both stages of development, total labeling in plasma was relatively stable over the same period of time.

Table 1 Lipid content of liver and plasma from 5-day-old (P5) and 14-day-old (P14) mice

Lipid		Liver		Plasma	
		P5 (nmoles/mg wet weight)	P14	P5 (nmoles/mL)	P14
CE	Total acyl chains	2.91 \pm 0.36	1.90 \pm 0.42*	1376 \pm 170	2057 \pm 154*
	DHA	0.05 \pm 0.01	0.02 \pm 0.01	43 \pm 7	66 \pm 8*
TAG	Total acyl chains	137.10 \pm 17.30	11.40 \pm 0.90*	6060 \pm 414	1870 \pm 80*
	DHA	3.00 \pm 0.30	0.40 \pm 0.01*	78 \pm 32	18 \pm 2*
FFA	Total fatty acids	1.80 \pm 0.50	1.30 \pm 0.20	577 \pm 82	418 \pm 104*
	DHA	0.03 \pm 0.01	0.04 \pm 0.00	16 \pm 1	5 \pm 1*
PL	Total acyl chains	68.90 \pm 2.10	89.00 \pm 1.30*	3925 \pm 81	4487 \pm 141*
	DHA	8.30 \pm 0.50	9.70 \pm 0.20*	214 \pm 9	188 \pm 11*
NL + PL	Total	209.30 \pm 17.60	102.60 \pm 1.30*	11938 \pm 280	8833 \pm 274*
	DHA	11.40 \pm 0.80	10.10 \pm 0.30*	352 \pm 48	277 \pm 21*
Ratio					
PL to TAG		0.75	11.71	0.97	3.50

Values are means \pm standard deviation of at least three separate determinations. Lipids were isolated by TLC, and fatty acids were derivatized to fatty acid methyl esters (FAME) for GLC quantification as detailed in Methods and materials. Cholesterol esters (CE), triacylglycerols (TAG), free fatty acids (FFA), phospholipids (PL), and neutral lipids (NL), total acyl chain content (Total), docosahexaenoic acid (DHA). Molar ratio calculation, PL to TAG: (Total μmole fatty acid in PL/2)/(Total mmole fatty acid in TAG/3). Statistically significant differences between P5 and P14 mice ($P < 0.05$, by Student's *t* test) are indicated (*).

Table 2 Changing acyl chain composition in lipids from liver in 5-day-old (P5) and 14-day-old (P14) mice

	P5			P14		
	CE	TAG	PL	CE	TAG	PL
Fatty Acid						
16:0	28.6 ± 4.3	19.0 ± 1.2	21.6 ± 0.3	30.4 ± 5.0	21.6 ± 3.6†	21.6 ± 2.6
18:0	8.3 ± 0.1	2.0 ± 0.4	16.8 ± 1.9	15.2 ± 3.1*†	7.9 ± 1.8*†	21.3 ± 0.6*†
Total Δ ₀	36.9	21.0	38.4	45.6	29.4	42.8
16:1n-7	5.8 ± 1.2	2.1 ± 0.2	0.5 ± 0.1	3.0 ± 1.5*†	0.5 ± 0.1*	0.2 ± 0.1*
18:1n-9	39.9 ± 1.2	39.6 ± 0.8	11.9 ± 0.5	36.0 ± 2.7	32.3 ± 1.4*†	7.4 ± 0.3*†
Total Δ ₁	45.7	41.8	12.4	39.0	32.8	7.6
18:2n-6	11.4 ± 2.1	22.3 ± 0.6	10.6 ± 0.8	11.8 ± 0.6	21.1 ± 1.2	13.5 ± 0.4*†
20:3	—	1.8 ± 0.1	1.4 ± 0.2	—	1.3 ± 0.1*	1.2 ± 0.1
20:4	3.3 ± 0.1	7.4 ± 0.5	22.2 ± 1.9	1.9 ± 0.8*	5.2 ± 0.5*	22.2 ± 1.4
22:4	1.7 ± 0.5	1.0 ± 0.0	0.7 ± 0.1	—	3.3 ± 0.2*	0.6 ± 0.1
22:5	—	0.6 ± 0.1	0.9 ± 0.1	—	1.6 ± 0.2*	0.7 ± 0.0
Total n-6	16.4	33.2	36.0	13.7	32.5	38.1
18:3n-3	—	0.6 ± 0.1	—	—	0.4 ± 0.4	—
20:5	—	0.6 ± 0.1	0.2 ± 0.0	—	—	0.2 ± 0.0
22:5	—	1.2 ± 0.3	1.0 ± 0.1	—	1.0 ± 0.0	0.4 ± 0.0*
22:6	1.6 ± 0.4	2.2 ± 0.1	12.1 ± 0.7	1.4 ± 0.5	3.3 ± 0.3*	11.0 ± 0.3*
Total n-3	1.6	4.6	13.3	1.4	4.7	11.6

Values are means ± standard deviation of at least three separate determinations and represent the mole percent content of the recovered acyl chains. Trace levels (—) and statistically significant differences between P5 and P14 mice ($P < 0.05$), by Student's *t* test (*) and by factorial analysis of variance (†) are indicated.

Table 3 Changing acyl chain composition in lipids from plasma in 5-day-old (P5) and 14-day-old (P14) mice

	P5			P14		
	CE	TAG	PL	CE	TAG	PL
Fatty Acid						
16:0	20.8 ± 4.9	31.1 ± 0.6	22.6 ± 2.4	14.6 ± 2.7†	35.2 ± 1.6*†	25.1 ± 1.3†
18:0	3.4 ± 2.9	2.9 ± 0.2	17.2 ± 0.4	1.8 ± 0.8	7.8 ± 0.4*†	22.1 ± 0.4*†
Total Δ ₀	22.4	34.0	39.8	16.4	43.0	47.2
16:1n-7	4.4 ± 1.0	4.6 ± 0.2	0.9 ± 0.2	1.9 ± 0.8	1.3 ± 0.3	0.2 ± 0.2
18:1n-9	19.8 ± 1.5	35.0 ± 3.0	10.0 ± 0.3	19.7 ± 1.6	34.5 ± 2.7	7.9 ± 0.7*
Total Δ ₁	24.2	39.6	10.6	21.6	35.8	8.1
18:2n-6	16.4 ± 2.1	13.7 ± 0.6	20.7 ± 0.4	29.5 ± 2.2*†	14.1 ± 0.4*	25.3 ± 0.7*†
18:3	0.9 ± 0.5	0.7 ± 0.3	0.3 ± 0.1	0.3 ± 0.2	0.3 ± 0.2	—
20:3	1.4 ± 0.5	0.8 ± 0.1	3.7 ± 0.3	1.4 ± 0.1	0.7 ± 0.0	3.2 ± 0.2
20:4	27.1 ± 4.2	6.5 ± 1.9	17.5 ± 2.2	26.6 ± 2.9	2.8 ± 0.3*†	10.4 ± 0.8*†
22:4	0.4 ± 0.3	0.7 ± 0.4	0.4 ± 0.1	—	0.6 ± 0.1	0.6 ± 0.1
22:5	0.3 ± 0.3	0.5 ± 0.2	0.4 ± 0.1	0.3 ± 0.3	0.5 ± 0.2	0.3 ± 0.1
Total n-6	46.5	22.6	43.0	58.1	19.0	39.8
18:3n-3	0.8 ± 0.2	0.8 ± 0.1	—	—	0.8 ± 0.3	—
20:5	1.0 ± 0.1	1.1 ± 0.4	0.5 ± 0.0	—	0.3 ± 0.1*	0.2 ± 0.1*
22:5	0.2 ± 0.1	0.6 ± 0.3	0.6 ± 0.1	—	0.2 ± 0.0*	0.3 ± 0.0*
22:6	3.2 ± 0.2	1.2 ± 0.5	5.2 ± 0.0	3.5 ± 0.4	0.9 ± 0.1	4.2 ± 0.2*
Total n-3	5.2	3.7	6.3	3.5	2.2	4.7

Values are means ± standard deviation of at least three separate determinations and represent mole percent of the total recovered for each acyl chain. Trace levels (—) and statistically significant differences between P5 and P14 mice ($P < 0.05$), by Student's *t* test (*) and by factorial analysis of variance (†) are indicated.

Plasma labeling decreased between 24 and 72 hr post-injection to approximately 50% of that at 24 hr. Moreover, plasma labeling at P5 was higher than labeling at P14 (2.2- and 1.5-fold higher at 2 and 72 hr post-injection, respectively). Based on linear regression analysis of the curves presented in *Figure 1*, the half-life of total [³H]DHA in liver and plasma was in P14 mice 1.6- and 1.9-times longer, respectively, than in P5 mice (*Table 5*). Both total PL and TAG displayed significantly higher half-lives at P14 than at P5 for both liver and plasma. In fact, minimal changes in TAG labeling

during the time course of this study at P14 did not allow accurate determination of its half-life, that was, nevertheless, greater than at P5. Differences in total [³H]DHA half-life are also correlated with the relative amounts of PL and TAG (*Table 1*) and the preferential esterification of [³H]DHA in PL at P14 (*Tables 5 and 6*).

In liver and plasma, developmental differences in the labeling of individual lipids as a function of time after injection indicated higher percent labeling of neutral lipids (NL) and lower percent labeling of PL at P5 compared with P14 (inserts,

Table 4 [³H]DHA accumulation in brain and retina is greater at postnatal day 14 (P14) than at postnatal day 5 (P5)

Time (hrs)	P5			P14		
	Liver	Brain	Retinas	Liver	Brain	Retinas
2	2.22 ± 0.09	0.03 ± 0.01	1.74 ± 0.26	2.76 ± 0.49	0.05 ± 0.00*	0.92 ± 0.13*
72	0.50 ± 0.08	0.44 ± 0.06	12.20 ± 0.83	1.10 ± 0.27*	1.03 ± 0.19*	17.60 ± 3.10*
Delta	-1.72	+0.41	+10.46	-1.66	+0.98	+16.68

Except for retinas where values are reported in nCi for two retinas (*n* > 3), all values represent total μCi of [³H]DHA recovered per organ and are means ± standard deviation of at least three separate determinations. P5 and P14 mice were injected with [³H]DHA (3.3μCi/g of body weight, i.p.) and killed 2 and 72hr later. Total amount of [³H]DHA injected was 12μCi/P5 pup and 20μCi/P14 pup. Delta is the difference between 72 and 2hr values. Statistically significant differences between P5 and P14 mice (*P* < 0.05, by Student's *t* test) are indicated (*).

Table 5 Half-life of [³H]DHA in total lipids, triacylglycerols (TAG), and phospholipids (PL) of liver and plasma from 5-day-old (P5) and 14-day-old (P14) mice

	P5					P14					P
	b	m ± S.E.	p	r ²	t _{1/2}	b	m ± S.E.	p	r ²	t _{1/2}	
Liver											
PL	1.13	-0.0086 ± 0.0005	<0.0001	0.94	35.0	1.01	-0.0071 ± 0.0006	<0.0001	0.91	42.4	0.0001
TAG	0.42	-0.0132 ± 0.0010	<0.0001	0.90	22.8	-0.23	-0.0043 ± 0.0009	<0.0004	0.66	70.0	0.0001
Total	1.23	-0.0964 ± 0.0007	<0.0001	0.92	31.4	1.04	-0.0069 ± 0.0006	<0.0001	0.91	43.5	0.0001
Plasma											
PL	0.50	-0.0056 ± 0.0005	<0.0001	0.87	53.8	0.30	-0.0044 ± 0.0009	<0.0006	0.67	68.4	0.0001
TAG	0.10	-0.0092 ± 0.0011	<0.0001	0.78	32.7	-0.71	-0.0037 ± 0.0020	<0.1120	0.27	81.4	0.0001
Total	0.72	-0.0059 ± 0.0003	<0.0001	0.96	51.0	0.41	-0.0036 ± 0.0007	<0.0003	0.67	83.6	0.0001

Half-lives (t_{1/2}) were estimated by a linear regression analysis; using the equation t_{1/2} = log 2.0/m, where m = slope of the curve. b is the y-intercept; p is the probability for the hypothesis H₀: slope (m) = 0; r², r-square, is the regression coefficient; P is the probability when testing the hypothesis that the slopes at P5 and P14 are equal.

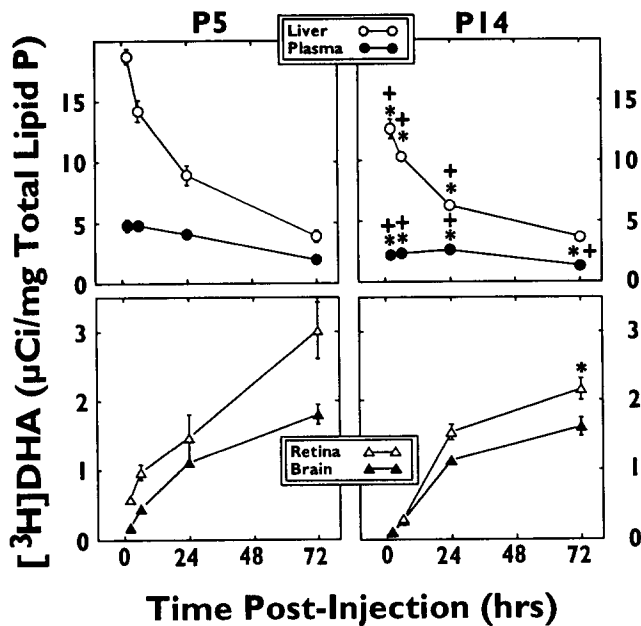


Figure 1 Time-dependent changes in [³H]DHA enrichment in plasma, liver, brain, and retina from 5-(P5) and 14-(P14) day-old mouse pups. Values in this and all subsequent figures are mean ± standard deviation of three to eight separate determinations. Statistically significant differences (*P* < 0.05) between P5 and P14 by Student's *t* test (*) and by factorial analysis of variance (+) are indicated.

Figure 2). In contrast to P14 mice, the P5 mice showed more rapid decrease in free hepatic [³H]DHA and TAG during the first 24 hr after injection. In both P5 and P14 mice, values for all these lipid classes showed similar labeling 72 hr post-injection. The labeling of total PL decreased as a function of time in both groups of mice with higher values at P5 during the first 24 hr after injection. Although total plasma labeling remained relatively constant during the first 24 hr after injection (*Figure 1*), significant differences were observed in the lipid distribution of [³H]DHA. As in the liver, plasma free DHA and TAG labeling decreased rapidly. In contrast, plasma PL labeling, where 90 to 92% of total [³H]DHA was esterified in phosphatidylcholine (PC, data not shown), showed a transient increase within the first 6 hr after injection in both P5 and P14 mice. In liver, [³H]DHA esterified in CE at all times examined after injection accounted for less than 0.6% of the total esterified [³H]DHA as compared with 3% and 9% in the plasma within 2 hr after injection. The labeling of CE increased in plasma during the first 24 hr after injection, when the total [³H]DHA labeling in plasma CE represented 15% at P5 and 20% at P14.

Striking similarities between the distribution of [³H]DHA in each lipid and the contribution of each lipid to the total endogenous DHA pool were evident (*Table 6*). TAG displayed a relatively higher labeling at P14 than at P5 in both liver (ratios: percent label to percent mass = 1.6 and 0.7, respectively) and plasma (ratios, 1.4 and 0.8, respectively).

Figure 3 depicts the labeling of liver phospholipids. Phosphatidylethanolamine (PE), followed by PC, was the most

Table 6 Endogenous DHA content and [³H]DHA in lipids of the liver and plasma from 5-day-old (P5) and 14-day-old (P14) mice

	P5		P14	
	DHA	[³ H]DHA	DHA	[³ H]DHA
Liver				
CE	0.40 ± 0.10	0.57 ± 0.08	0.27 ± 0.04	0.34 ± 0.05*
TAG	26.50 ± 0.70	18.00 ± 3.30	3.70 ± 0.10*	5.90 ± 0.03*
FFA	0.28 ± 0.05	1.26 ± 0.05	0.47 ± 0.16	0.35 ± 0.05*
PL	72.90 ± 0.50	78.70 ± 5.00	95.80 ± 0.20*	93.10 ± 0.23*
PL/TAG	2.8	4.4	25.9	15.8
Plasma				
CE	12.30 ± 0.30	17.00 ± 1.10	23.78 ± 1.07*	19.50 ± 1.60
TAG	21.48 ± 6.14	16.30 ± 2.50	6.47 ± 0.49*	9.20 ± 0.80*
FFA	4.72 ± 0.51	3.70 ± 0.90	1.90 ± 0.40*	2.60 ± 0.30
PL	61.38 ± 5.85	60.70 ± 2.10	67.86 ± 1.13*	65.80 ± 2.90*
PL/TAG	2.9	3.7	10.5	7.2

Values are means ± standard deviation of at least three separate determinations and represent percent contribution of specific DHA-lipids to total endogenous DHA and percent distribution of [³H]DHA with respect to total radioactivity recovered at the time of maximal labeling in the liver (2 hr after injection), and in plasma (24 to 72 hr after injection), when time-dependent changes in labeling distribution were minimal. Statistically significant differences between P5 and P14 mice (*P*<0.05, by Student's *t* test) are indicated (*).

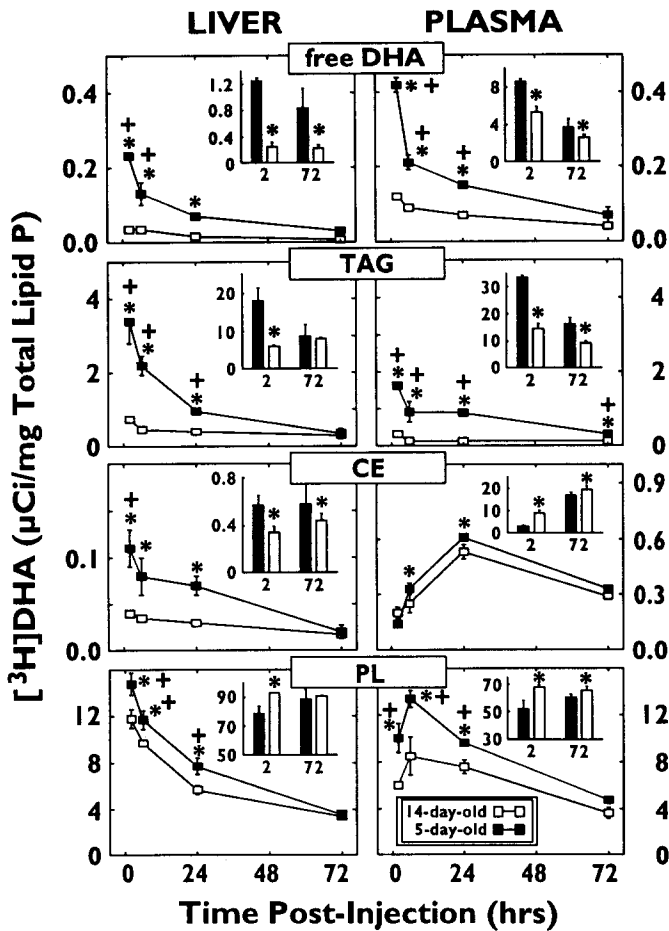


Figure 2 Changes in [³H]DHA lipid labeling as a function of time in liver and plasma from P5 and P14 mice. The percent contribution of [³H]DHA in lipids at 2 and 72 hr after injection and statistical significance by Student's *t* test (*) are shown in the insets. Free fatty acids (FFA), cholesterol esters (CE), triacylglycerols (TAG), phospholipids (PL). Other details as in Figure 1.

highly labeled phospholipid in both ages of mice. Within the first 6 hr post-injection, PE labeling decreased by 35%, while phosphatidylserine (PS) and PC labeling increased. Within 72 hr post-injection, PE labeling was decreased by 80%, whereas only 64% of the maximum labeling in PC was lost. As seen in Figure 3, PC was the only phospholipid with similar labeling at both postnatal ages.

[³H]DHA uptake by brain and retina

Both retina and brain showed increases in [³H]DHA labeling as a function of time after injection (Table 4). However, the labeling was higher in the retina than in the brain at both developmental stages (Figure 1). Furthermore, 80 to 90% of the total recovered [³H]DHA was esterified in PL (data not shown). Postnatal differences in plasma [³H]DHA content could contribute to the higher brain and retina labeling seen in P5 as compared with P14 pups. In fact, the ratio of brain and retina to plasma labeling revealed that the uptake at P14 was proportionally higher than in mice injected at P5 (Figure 4). The values thus obtained showed reduced statistical variation (standard deviation) and resulted in more linear rates of [³H]DHA incorporation into brain and retina than the values obtained by simply plotting the uptake of [³H]DHA in brain and retina as a function of time.

Discussion

This study shows that the degree to which i.p.-injected [³H]DHA is taken up and esterified in phospholipids in liver, brain, and retina is dependent on postnatal developmental age. The profile of [³H]DHA labeling in liver lipids reflects that of the endogenous DHA content. At P5, endogenous content and [³H]DHA labeling of TAG is higher than that at P14. Conversely, in P14 mice, the [³H]DHA labeling of PL is greater. The esterification of [³H]DHA in the plasma PL and TAG closely reflects that of the liver, and more efficient accumulation of DHA in the retina and brain is seen at P14. This is correlated with preferential esterification

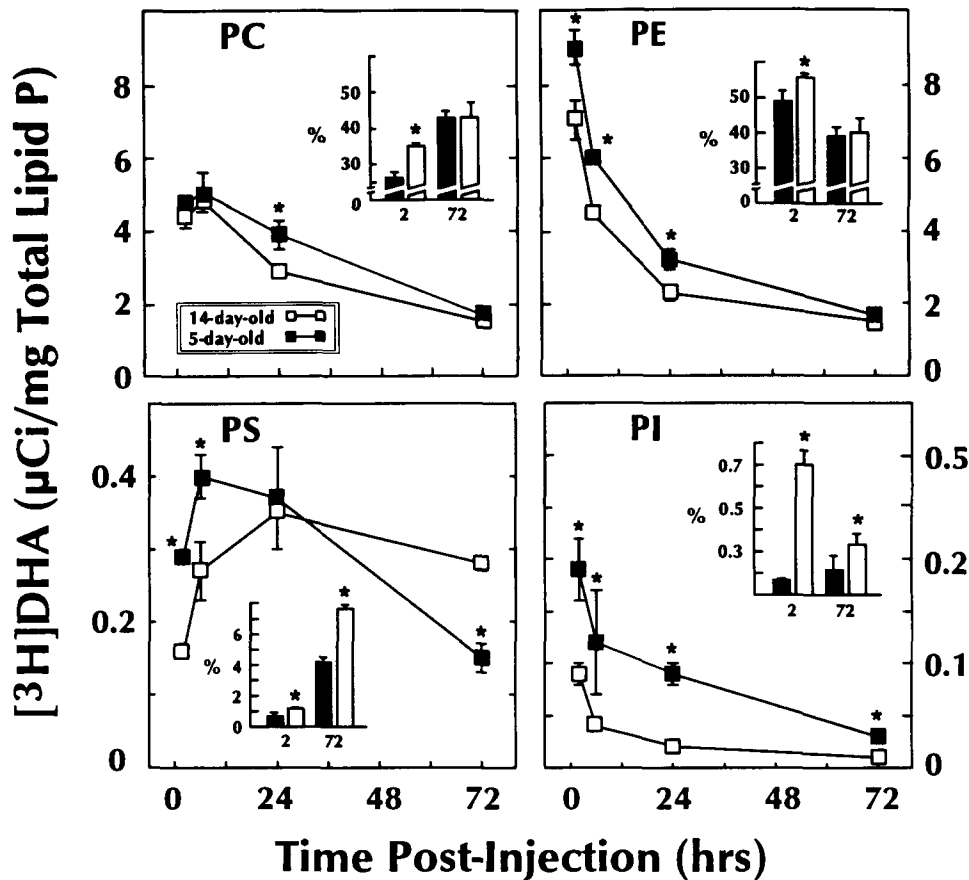


Figure 3 Time-dependent changes in distribution of total $[^3\text{H}]\text{DHA}$ label in phospholipids of livers from 5- and 14-day-old mouse pups. The percent contribution of $[^3\text{H}]\text{DHA}$ in each lipid to the total is shown in the inset. (*): $P < 0.05$ by Student's t test. Phosphatidylcholine (PC), phosphatidylethanolamine (PE), phosphatidylserine (PS), phosphatidylinositol (PI).

of DHA into PL and a higher half-life of DHA-PL both in liver and plasma. It is important to note that increased DHA esterification into PL coincides with the periods of murine photoreceptor biogenesis and synaptogenesis.^{47,48}

The livers of younger mice were enriched in TAG, with a molar ratio PL to TAG = 0.8 at P5 and 11.7 at P14. A rapid increase in liver TAG that takes place in rat pups within the first 24 hours of postnatal life^{49,50} is related to the transition from a diet rich in carbohydrate during fetal life to a fat-rich diet during the suckling period. Along with this change in diet, plasma glucagon levels peak immediately after birth⁵¹ and stimulate hepatic storage of dietary fatty acids into TAG.³⁴ Compared with P5 mice, the hepatic content of TAG was drastically reduced at P14 ($\approx 90\%$), and PL was enriched. A similar decrease in TAG content, approaching levels reported in mature rats, has been reported for rats between postnatal day 1 and day 10.⁵¹ Also, cultured hepatocytes from adult rats display higher capacity for TAG synthesis and secretion than those of P6 and P12 rat pups.⁵² Moreover, TAG synthesis is more active in hepatocytes from P6 mice than in those from P12, and TAG release to the medium is proportional to cellular synthesis (higher at P6 than at P12). Taken together, these findings suggest that there is an early postnatal period of rapid TAG synthesis

and accumulation in the liver, followed by a transient shift toward PL synthesis prior to weaning, when the change to a carbohydrate-rich diet stimulates TAG synthesis and secretion.³⁴ The factor(s) responsible for these early postnatal changes in hepatic lipid metabolism are not known. One possibility could be down-regulation of glucagon receptors due to a sustained postnatal hyperglucagonaemia,³⁴ thus reducing hormonal-stimulated TAG synthesis.

The initial high incorporation of $[^3\text{H}]\text{DHA}$ into phosphatidylethanolamine (PE) and the subsequent fast decrease in its labeling concomitant with a slow increase of phosphatidylcholine (PC) labeling (after 6 hr) suggest that N-methylation of DHA-PE is involved in the formation of DHA-PC in the liver of mouse pups. This pathway, reported in rat hepatocytes,⁵³ has been suggested as the mechanism for the delivery of DHA to developing tissue.⁵⁴

Within this complex scenario of changing hepatic metabolism during postnatal life, the endogenous DHA-lipid content and $[^3\text{H}]\text{DHA}$ esterification followed similar trends. In P5 mice, TAG showed a higher contribution to total DHA mass (26.5%) and total $[^3\text{H}]\text{DHA}$ labeling (18%) than in P14 mice (3.7 and 5.9%, respectively) (Table 6). Two hours after $[^3\text{H}]\text{DHA}$ administration, the livers of P5 mice showed a more efficient uptake than at P14 (19% versus 14% of the injected

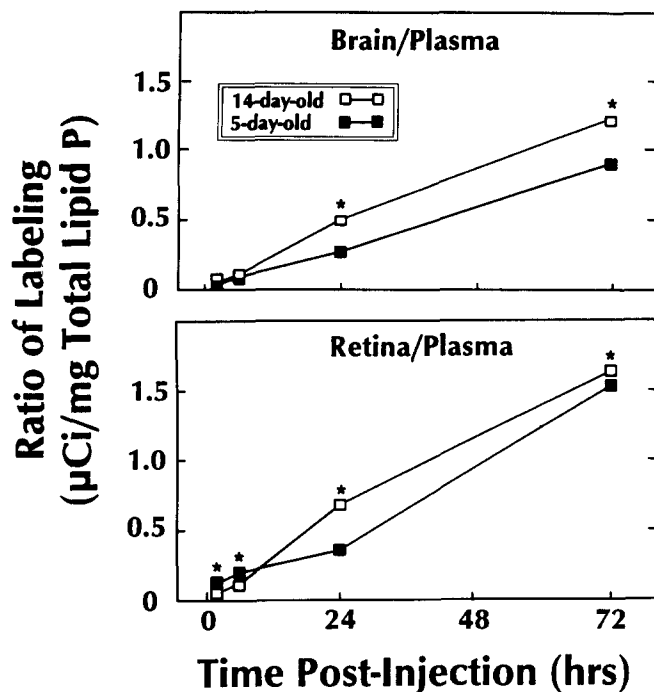


Figure 4 Time dependent changes in $[^3\text{H}]\text{DHA}$ enrichment in brain and retina from 5- and 14-day-old mouse pups. Values shown are the ratio of labeling ($\mu\text{Ci}[^3\text{H}]\text{DHA}/\text{mg}$ lipid P) in the retina and brain to plasma. (*): $P < 0.05$ by Student's t test.

dose), and the precursor was actively esterified in PL and TAG. By comparing mass and labeling distribution, it became apparent that the high labeling of TAG at P5 may be the consequence of a shift in the *de novo* pathway of lipid synthesis, which favors TAG. Proportionally more active labeling of TAG was observed at P5 (Table 6), and this is representative of the higher percent content of DHA in TAG at this age (Table 2). Interestingly, at P5 the DHA content of maternal milk is much higher than at P14,²⁷ and, therefore, the liver appears to be developmentally more prepared to take up dietary DHA efficiently and sequester any surplus into a TAG reservoir. By day 14, as the hepatic activity of Δ -6 desaturase peaks,³² the liver can also utilize 18:3n-3 more efficiently to support its own needs for DHA and the needs of other tissues, such as retina, that require DHA for membrane synthesis.⁴⁸ Thus, during the suckling period, the liver is preferentially involved in taking up DHA or its precursors and secreting DHA esterified in PL and TAG into the plasma: (a) the developmental changes in DHA mass and lipids labeling observed in the liver (above) were also seen in plasma; (b) less than $0.5 \mu\text{Ci}$ of $[^3\text{H}]\text{DHA}$ was present in whole plasma 2 hr after injection, while the liver contained 2.2 to 2.8 μCi ; (c) the ratio of 18:3n-3 to 22:6n-3 is higher in the stomach (approximately 2.0) than in the plasma (approximately 0.9);²⁷ (d) 18:3n-3 is elongated and desaturated in the liver of P3 mice before $[^{14}\text{C}]22:6\text{n-3}$ appears in the PL and TAG of plasma;²⁷ and (e) in both this study and that of Scott and Bazan,²⁷ radiolabeled DHA accumulated in the liver prior to accumulation in the brain and retina.

Therefore, developmental differences between individual plasma lipid pools reflect changes in hepatic lipid metabolism. Further analysis of lipoproteins will provide relevant

information about the characteristics of nascent lipoproteins (apoprotein and lipid composition) that can be related, at least in part, to the efficiency of the system supplying the DHA to brain and retina. Chylomicrons and very low density lipoproteins (VLDL) are enriched in TAG. However, during the suckling period, the murine liver has limited capability for the assembly or secretion of nascent VLDL-TAG.⁵⁵ Also, lower hepatic synthesis of TAG at P14 could lead to the output of lipoproteins with higher PL to TAG ratios that are more dense and smaller in size⁵⁶ than at P5. Because an increase in the size of a lipoprotein particle is positively correlated with its utilization by peripheral tissues,³⁴ the smaller size of lipoprotein particles at P14 could favor their transport to the CNS and, therefore, lead to the more efficient delivery of DHA observed in this study.

A significant proportion of plasma DHA (higher at P5 than at P14) was found as free DHA. Although most of the labeling appeared esterified in plasma lipids, hepatic secretion of free DHA and lysophospholipids,³³ bound to albumin or other serum proteins such as alpha-fetoprotein and fetuin,⁵⁷ may also contribute to the delivery of DHA to the CNS and other peripheral organs. In fact, after the delivery of $[^{14}\text{C}]\text{DHA}$ into the stomach of young adult rats as a complex with albumin, there is an early labeling of chylomicron/VLDL followed by labeling of intermediate and low density lipoproteins (LDL).⁵⁸ A small proportion of $[^{14}\text{C}]\text{DHA}$ is also associated with albumin and another unidentified plasma protein. As observed in the present study and in those of Scott and Bazan²⁷ and Li et al.,⁵⁸ hepatic DHA labeling peaked early and was followed by accumulation of labeling in the retina. This evidence further suggests that the output of DHA from the liver (either free or esterified) is an important preceding step for the efficient uptake of DHA by the retina and brain.

The role of CE in DHA transport and its origin in plasma also deserves consideration. In the present study, CE was the only lipid that: (a) displayed higher percent DHA content in plasma (Table 3) as compared with liver (Table 2); (b) showed an increased contribution (nmole/mL) to total plasma DHA at P14 when compared with P5 (Table 1); (c) was labeled to a similar extent in plasma at both ages, while labeling of other lipids was considerably higher at P5 than at P14 (Figure 2); and (d) became more enriched in $[^3\text{H}]\text{DHA}$ labeling in plasma for up to 24 hours when its percent contribution to total $[^3\text{H}]\text{DHA}$ reached maximal values (17 to 19%) (Figure 2). The synthesis of CE in the liver and its incorporation into nascent VLDL accounts for only a small proportion of total plasma CE. The bulk of CE is synthesized in high density lipoprotein (HDL) by lecithin-cholesterol acyltransferase (LCAT), which cleaves the fatty acids in the C_2 position of PC and transfers them to cholesterol.³³ The association of LCAT with a cholesteryl ester transfer protein (CETP) facilitates the shift of CE from HDL to other lipoproteins (LDL and VLDL). This process is very active in humans as well as frogs, but it is minimal in other species, i.e., rats, which lack CETP.⁵⁹ The majority of CE present in VLDL is incorporated in nascent VLDL by hepatocytes, while in LDL as much as 40% is derived from HDL.⁶⁰ Therefore, in animals with low CETP activity, HDL will not only carry CE from the periphery to the liver for degradation but also transport cholesterol to support other tissues' needs.³³ If mice, like rats, lack CETP, analysis of DHA content and $[^3\text{H}]\text{DHA}$ labeling in CE of VLDL, LDL,

and HDL could provide relevant information about both synthesis and secretion of [³H]DHA-CE by the liver and/or its synthesis in HDL from a highly labeled [³H]DHA-PC pool. In this context, it is of interest to mention that the content of DHA in HDL obtained from suckling rats is higher than that of VLDL-LDL lipoproteins.³⁸

Whatever the origin of plasma CE (either liver or HDL), our results clearly show that DHA-CE accounts for a significant proportion of DHA in plasma of suckling mice both in mass (16 to 30% of total, *Table 6*) and in labeling (17 to 20% of the total, *Table 6*). Similar values were reported in P5 mice after [³H]DHA injection.¹¹ High labeling of plasma CE also occurs in frogs following administration of [³H]DHA, and the labeling ratio of CE to PC reflected their 1:1 molar contribution to circulating DHA.⁴⁰ Further analysis is necessary to evaluate the potential role of DHA-CE as a carrier of DHA to the CNS and other tissues. Moreover, mRNA expression for apoD in tissues of rhesus monkey revealed that this apoprotein, involved in CE transport, is not only present in an HDL complex with LCAT but also in tissues such as brain, mainly in perivascular areas.⁶¹ These authors suggest that apoD may be involved in the influx and efflux of cholesterol and CE across the blood-brain barrier. If this mechanism operates in brain and retina, it may play an important role in the supply of cholesterol, as well as of DHA to the CNS, both of which are needed during neural cell membrane biogenesis.

In summary, this study shows that hepatic DHA uptake is very active in suckling rats and higher than that observed using its precursor 18:3n-3 (8% of the dose).²⁷ The subsequent esterification in hepatic lipids for lipoprotein assembly and secretion seems to be developmentally regulated with a tendency for more active synthesis of [³H]DHA-TAG at P5 and of [³H]DHA-PL at P14. Despite differences in [³H]DHA esterification between TAG (mainly an energy source) and PL (mainly structural lipids), the fast decrease of liver labeling during the 24 hours postinjection was similar for both P5 and P14 (-52%) and lower than the one observed with [¹⁴C]18:3n-3 (-70%).^{27,40} It appears that the formation of DHA-TAG at P5 is linked to its secretion into nascent lipoproteins rather than to its utilization in oxidative pathways. This is supported by a similar higher mass and labeling contribution of DHA-TAG to circulating plasma DHA at P5 as compared with P14. Although no labeling was detected by HPLC analysis in other fatty acid products of partial DHA oxidation, DHA may be oxidized to acid soluble products. Experiments done in rats after oral administration of [¹⁴C]-labeled fatty acids indicated that C18 fatty acids (i.e., 18:1n-9, 18:3n-3) are preferentially oxidized over C20 polyunsaturated ones (20:3n-6, 20:4n-6).⁶² It appears logical that the liver (and other organs) will preserve polyunsaturated fatty acids (PUFA) (i.e., DHA) to support the demands for cell growth and development while using other saturated and monoenoic fatty acids (abundant in the milk fat) as an energy source.

The efficiency of administered [³H]DHA to reach the CNS by 72 hours postinjection (3.5 and 5% of the administered dose at P5 and P14, respectively) was much higher than that obtained with [¹⁴C]18:3n-3 (0.5% of the dose),⁴⁰ a PUFA that is actively oxidized.^{40,62} The increase in brain and retina labeling as a function of time after injection, concomitant with the decrease of hepatic lipids labeling, strongly suggests that hepatic secretion of lipoproteins with high DHA-PL to DHA-

TAG ratios favors the accumulation of DHA in brain and retina. Moreover, the potential contribution of DHA-CE as a quantitatively smaller (than PL) carrier of DHA to neuronal tissues may involve its synthesis in plasma HDL from hepatically derived DHA-PC pool and/or in the liver.

Acknowledgments

We thank Feng Cai for his contribution during early stages of this work and Nilda Parkins and Fannie Richardson for technical assistance.

References

- 1 Aveldaño de Caldironi, M.I. and Bazan, N.G. (1980). Composition and biosynthesis of molecular species of retina phosphoglycerides. *Neurochem. Int.* **1**, 381-392
- 2 Fliesler, S.J. and Anderson, R.E. (1983). Chemistry and metabolism of lipids in the vertebrate retina. *Prog. Lipid Res.* **22**, 79-131
- 3 Sun, G.Y. and Sun, A.Y. (1972). Phospholipids and acylgroups of synaptosomal and myelin membranes isolated from the cerebral cortex of squirrel monkey (*Saimiri sciureus*). *Biochim. Biophys. Acta* **280**, 306-315
- 4 Poulos, A., Darin-Bennett, A., and Shite, I.G. (1973). The phospholipid-bound fatty acids and aldehydes of mammalian spermatozoa. *Comp. Biochem. Physiol.* **46B**, 541-549
- 5 Neuringer, M., Conner, W.E., Van Petten, C., and Barstad, L. (1984). Dietary omega-3 fatty acid deficiency and visual loss in infant Rhesus monkeys. *J. Clin. Invest.* **73**, 272-276
- 6 Neuringer, M., Anderson, G.J., and Connor, W.E. (1988). The essentiality of n-3 fatty acids for the development and function of the retina and brain. *Ann. Rev. Nutr.* **8**, 517-541
- 7 Uauy, R.D., Birch, D.G., Birch, E., Tyson, J.E., and Hoffman, D.R. (1990). Effect of omega-3 fatty acids on retinal function in very low birth weight infants. *Pediatric Res.* **28**, 485-492
- 8 Anderson, G.J., Connor, W.E., and Corliss, J.D. (1990). Docosahexaenoic acid is the preferred dietary n-3 fatty acid for the development of the brain and retina. *Pediatric Res.* **27**, 89-97
- 9 Innis, S.M. (1991). Essential fatty acids in growth and development. *Prog. Lipid Res.* **30**, 39-103
- 10 Uauy, R., Birch, E., Birch, D., and Peirano, P. (1992). Visual and brain function measurements in studies of n-3 fatty acid requirements of infants. *J. Pediatr.* **120**, S168-S180
- 11 Martin, R.M. and Bazan, N.G. (1992). Changing fatty acid content of growth cone lipids prior to synaptogenesis. *J. Neurochem.* **59**, 318-325
- 12 Bazan, N.G., Rodriguez de Turco, E.B., Gordon, W.C., and Parkins, N.E. (1993). Light stimulates docosahexaenoic acid (DHA) metabolism and mobilization in the liver: evidence for an eye to liver signal. *ARVO Abstract Invest. Ophthalm. Vis. Sci. (Suppl)* **34**, 1329
- 13 Wheeler, T.G., Bendken, R.M., and Anderson, R.E. (1975). Visual membranes: Specificity of fatty acid precursors for the electrical response to illumination. *Science* **188**, 1312-1314
- 14 Neuringer, M. and Connor, W.E. (1986). Omega-3 fatty acids in the brain and retina: evidence for their essentiality. *Nutr. Rev.* **44**, 285-294
- 15 Bourre, J.M., Bonneil, M., Dumont, O., Picotti, M.J., Pascal, G.A., and Durand, G.A. (1989). The effects of dietary α -linolenic acid on the composition of nerve membranes, enzymatic activity, amplitude of electrophysiological parameters, resistance to poisons and performance of learning tasks. *J. Nutr.* **119**, 1880-1892
- 16 Lamptey, M.S. and Walker, B.L. (1976). A possible essential role for dietary linolenic acid in the development of the young rat. *J. Nutr.* **106**, 86-93
- 17 Yamamoto, N., Hashimoto, A., Takemoto, Y., Okuyama, H., Nomura, M., Kitajima, R., Togashi, T., and Tamai, Y. (1988). Effect of dietary alpha linolenate/linoleate balance on lipid composition and learning ability of rats. *J. Lipid Res.* **29**, 1013-1021
- 18 Simopoulos, A.P. (1991). Omega-3 fatty acids in health and disease and in growth and development. *Am. J. Clin. Nutr.* **54**, 438-463

- 19 Tinoco, J. (1982). Dietary requirements and functions of α -linolenic acid in animals. *Prog. Lipid Res.* **21**, 1–45
- 20 Nettleton, J.A. (1991). ω -3 fatty acids: comparison of plant and seafood sources in human nutrition. *J. Am. Dietetic Assoc.* **91**, 331–337
- 21 Clark, K.J., Makrides, M., Neuman, M.A., and Gibson, R.A. (1992). Determination of the optimal ratio of linoleic acid to α -linolenic acid. *J. Pediatr.* **120**, S150–S158
- 22 Wainwright, P.E., Huang, Y.S., Bulman-Fleming, B., Dalby, D., Mills, D.E., Redden, P., and McCutcheon, D. (1992). The effects of dietary n-3/n-6 ratio on brain development in the mouse: A dose response study with long chain n-3 fatty acids. *Lipids* **27**, 98–103
- 23 Wetzel, M.G., Li, J., Alvarez, R.A., Anderson, R.E., and O'Brien, P.J. (1991). Metabolism of linolenic acid and docosahexaenoic acid in rat retinas and rod outer segments. *Exp. Eye Res.* **53**, 437–446
- 24 Moore, S.A., Yoder, E., Murphy, S., Dutton, G.R., and Spector, A.A. (1991). Astrocytes not neurons produce docosahexaenoic acid (22:6 ω -3) and arachidonic acid (20:4 ω -6). *J. Neurochem.* **56**, 518–524
- 25 Bazan, H.E.P., Careaga, M.M., Sprecher, H., and Bazan, N.G. (1982). Chain elongation and desaturation of eicosapentaenoate to docosahexaenoate and phospholipid labeling in the rat retina in vivo. *Biochim. Biophys. Acta* **712**, 123–128
- 26 Cook, H.W. (1978). In vitro formation of polyunsaturated fatty acids by desaturation in rat brain: some properties of the enzymes in developing brain and comparisons with liver. *J. Neurochem.* **30**, 1327–1334
- 27 Scott, B.L. and Bazan, N.G. (1989). Membrane docosahexaenoate is supplied to the developing brain and retina by the liver. *Proc. Natl. Acad. Sci. U.S.A.* **86**, 2903–2907
- 28 Stinson, A.M., Wiegand, R.D., and Anderson, R.E. (1991). Recycling of docosahexaenoic acid in rat retinas during n-3 fatty acid deficiency. *J. Lipid Res.* **32**, 2009–2017
- 29 Wiegand, R.D., Koutz, C.A., Stinson, A.M., and Anderson, R.E. (1991). Conservation of docosahexaenoic acid in rod outer segments of rat retina during n-3 and n-6 fatty acid deficiency. *J. Neurochem.* **57**, 1690–1699
- 30 Bazan, N.G., Gordon, W.C., and Rodriguez de Turco, E.B. (1992). Docosahexaenoic acid uptake and metabolism in photoreceptors: Retinal Conservation by an efficient retinal pigment epithelial cell-mediated recycling process. In *Neurobiology of Essential Fatty Acids*, (N.G. Bazan, M. Murphy, and E. Toffano, eds.), p. 295–306, Plenum Press, New York, NY USA
- 31 Bourre, J.-M.E., Dumont, O.S., Picotti, M.J., Pascal, G.A., and Durand, G.A. (1992). Dietary α -linolenic acid deficiency in adult rats for 7 months does not alter brain docosahexaenoic acid content, in contrast to liver, heart and testes. *Biochim. Biophys. Acta* **1124**, 119–122
- 32 Bourre, J.M. and Picotti, M. (1992). Delta-6 desaturation of alpha-linolenic acid in brain and liver during development and aging in the mouse. *Neurosci. Lett.* **141**, 65–68
- 33 Vance, J.E. and Vance, D.E. (1990). Lipoprotein assembly and secretion by hepatocytes. *Annu. Rev. Nutr.* **10**, 337–356
- 34 Gibbons, G.F. (1990). Assembly and secretion of hepatic very low density lipoprotein. *Biomedical J.* **268**, 1–13
- 35 Bazan, N.G., Birkle, D., and Reddy, T.S. (1985). Biochemical and nutritional aspects of the metabolism of polyunsaturated fatty acids and phospholipids in experimental models of retinal degenerations. In *Retinal Degeneration: Experimental and Clinical Studies*, (M.M. LaVail, M. Anderson, and J. Hollyfield, eds.), p. 159–187, Alan R. Liss, Inc., New York, NY USA
- 36 Bazan, N.G. (1989). The identification of new biochemical alteration early in the differentiation of visual cells in inherited retinal degenerations. In *Inherited and Environmentally Induced Retinal Degenerations*, p. 191–215, Alan R. Liss, New York, NY USA
- 37 Bazan, N.G. (1990). Supply of n-3 polyunsaturated fatty acids and their significance in the central nervous system. In *Nutrition and the Brain*, Vol. 8, (R.J. Wurtman and J.J. Wurtman eds.), p. 1–24, Raven Press, New York, NY USA
- 38 Nouvelot, A., Delbart, C., and Bourre, J.M. (1986). Hepatic metabolism of alpha-linolenic acid in suckling rats and its possible importance in polyunsaturated fatty acid uptake by the brain. *Ann. Nutr. Metab.* **30**, 316–323
- 39 Bazan, N.G., Reddy, T.S., Redmond, T.M., Wiggert, B., and Chader, G.J. (1985). Endogenous fatty acids are covalently and non-covalently bound to interphotoreceptor retinoid-binding protein in the monkey retina. *J. Biol. Chem.* **260**, 13677–13680
- 40 Bazan, N.G., Rodriguez de Turco, E.B., and Gordon, W.C. (1993). Pathways for uptake and conservation of docosahexaenoic acid in photoreceptors and synapses: Biochemical and autoradiographic analysis. *Can. J. Physiol. Pharmacol.* **71**, 690–698
- 41 Marcheselli, V.L. and Bazan, N.G. (1990). Quantitative analysis of fatty acids in phospholipids, diacylglycerols, free fatty acids, and other lipids. *J. Nutr. Biochem.* **1**, 382–388
- 42 Rouser, G., Fleischer, S., and Yamamoto, A. (1970). Two-dimensional thin layer chromatographic separation of polar lipids and determination of phospholipids by phosphorus analysis of spots. *Lipids* **5**, 494–496
- 43 Marcheselli, V.L., Scott, B.L., Reddy, T.S., and Bazan, N.G. (1988). Quantitative analysis of acyl group composition of brain phospholipids, neutral lipids, and free fatty acids. In *Neuromethods, Vol 7: Lipids and Related Compounds*, (A.A. Boulton, G.B. Baker, and L.A. Horrocks, eds), p. 83–110, Humana Press, Totowa, NJ USA
- 44 Snedecor, G.W. and Cochran, W.G. (1980). *Statistical Methods*, 7th Edition, Iowa State University Press, Ames, IA USA
- 45 SAS Institute (1987). *SAS/STAT Guide for Personal Computers*, Version 6 Edition, p. 519–640, SAS Institute, Cary, NC USA
- 46 Freund, R.J., Littell, R.C., and Spector, P.C. (1986). *SAS System for Linear Models*, 1986 Edition, SAS Institute, Cary, NC USA
- 47 Scott, B.L., Reddy, T.S., and Bazan, N.G. (1987). Docosahexaenoate metabolism and fatty-acid composition in developing retinas of normal and *rd* mutant mice. *Exp. Eye Res.* **44**, 101–113
- 48 Scott, B.L., Racz, E., Lolley, R.N., and Bazan, N.G. (1988). Developing rod photoreceptors from normal and mutant *rd* mouse retinas: Altered fatty acid composition early in development of the mutant. *J. Neurosci. Res.* **20**, 202–211
- 49 Sinclair, A.J. (1974). Fatty acid composition of liver lipids during development of rat. *Lipids* **9**, 809–818
- 50 Jamdar, S.C., Moon, M., Bow, S., and Fallon, H.J. (1978). Hepatic lipid metabolism. Age related changes in triglyceride metabolism. *J. Lipid Res.* **19**, 763–770
- 51 Mangeny, M., Cardot, P., Lyonnet, S., Coupe, C., Benarous, R., Munnich, A., Girard, J., Chambaz, J., and Bereziat, G. (1989). Apolipoprotein-E gene expression in rat liver during development in relation to insulin and glucagon. *Eur. J. Biochem.* **181**, 225–230
- 52 Coleman, R.A., Haynes, E.B., Sand, T.M., and Davis, R.A. (1988). Developmental and coordinate expression of triacylglycerol and small molecular weight apo B synthesis and secretion by rat hepatocytes. *J. Lipid Res.* **29**, 33–42
- 53 Samborski, R.W., Ridgway, N.D., and Vance D.E. (1990). Evidence that only newly made phosphatidylethanolamine is methylated to phosphatidylcholine and that phosphatidylethanolamine is not significantly deacylated-reacylated in rat hepatocytes. *J. Biol. Chem.* **265**, 18322–18328
- 54 Burdge, G.C., Kelly, F.J., and Postle, A.D. (1993). Mechanisms of hepatic phosphatidylcholine synthesis in the developing guinea pig: contributions of acyl remodeling and of N-methylation of phosphatidylethanolamine. *Biochem. J.* **290**, 67–73
- 55 Frost, S.C., Clark, W.A., and Wells, M.A. (1983). Studies on fat digestion, absorption and transport in the suckling rat IV. In vivo rates of triacylglycerol secretion by intestine and liver. *J. Lipid Res.* **24**, 899–903
- 56 Zhang, Z.J., Wilcox, H.G., Elam, M.B., Castellani, L.W., and Heimberg, M. (1991). Metabolism of n-3 fatty acids by the isolated perfused rat liver. *Lipids* **26**, 504–511
- 57 Subbiah, M.T.R. (1991). Newly recognized lipid carrier proteins in fetal life. *Proc. Soc. Exp. Biol. Med.* **198**, 495–499
- 58 Li, J., Wetzel, M.G., and O'Brien, P. (1992). Transport of n-3 fatty acids from the intestine to the retina in rats. *J. Lipid Res.* **33**, 539–548
- 59 Oschry, V. and Eisenberg, S. (1982). Rat plasma lipoproteins: reevaluation of a lipoprotein system in an animal devoid of cholesteryl ester transfer activity. *J. Lipid Res.* **23**, 1099–1106
- 60 Fielding, P.E. and Fielding, C.J. (1991). Dynamics of lipoprotein transport in the circulatory system. In *New Comprehensive Biochemistry, Vol. 20. Biochemistry of Lipids, Lipoproteins and Membranes*, (D.E. Vance and C.J. Vance, eds), p. 427–459, Elsevier, New York, NY USA
- 61 Smith, K.M., Lawn, R.M., and Wilcox, J.N. (1990). Cellular localization of apolipoprotein D and lecithin: Cholesterol acyltransferase mRNA in rhesus monkey tissue by in situ hybridization. *J. Lipid Res.* **31**, 995–1004
- 62 Leyton, J., Drury, P.J., and Crawford, M.A. (1987). In vivo incorporation of labeled fatty acids in rat liver lipids after oral administration. *Lipids* **22**, 553–558